Electronic Supplementary Material (ESI) for RSC Applied Polymers.

Electronic Supplementary Information

A new multifunctional energy harvester based on mica nanosheets-dispersed PVDF nanofabrics featuring piezo-capacitive, piezoelectric and triboelectric effects

Govind S. Ekbote[1], Mohammed Khalifa[2], B. Venkatesa Perumal[3], S. Anandhan[1]

[1] Department of Metallurgical and Materials Engineering, National Institute of Technology Karnataka, Srinivas nagar, Mangaluru 575025, India.
[2] Kompetenzzentrum Holz GmbH, W3C, A-9300 St. Veit/Glan, Klagenfurter Strasse 87-89, Linz, Austria.
[3] Department of Electrical and Electronics Engineering, National Institute of Technology Karnataka, Srinivas nagar, Mangaluru 575025, India.

1. Piezoelectric and piezo capacitive device

The copper tape adhered to the flexible insulating plastic sheet served as the electrode for the piezo capacitance test. The PVDF/MNS-0.75 composite nanofabric (12 mm × 12 mm) was placed between the electrodes. The electrode edges were cushioned with a thin thermoplastic polyurethane (TPU) layer. It does not contribute to the piezo capacitive performance of the device (Figure S1(a)). A similar setup was constructed for piezoelectric measurements without TPU, as shown in Figure S1(b).

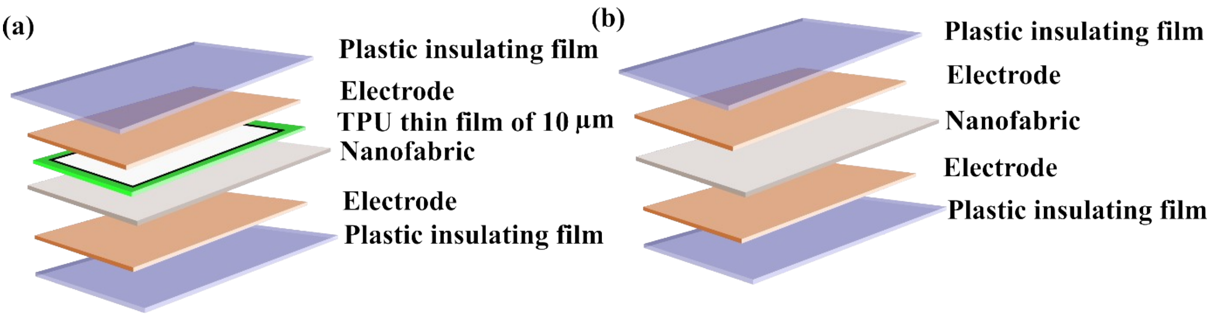

Figure. S1 Setup used to evaluate (a) Piezo-capacitance based pressure sensor, (b) Piezoelectric nanogenerator.

2. Surface roughness measurement of Cu tape/Cu electrode

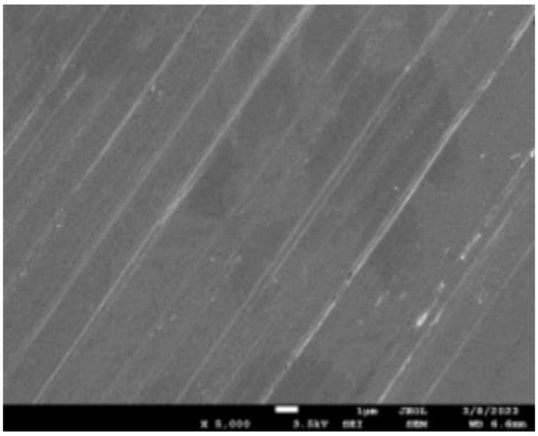

Figure. S2 FESEM image of the surface of the copper tape.

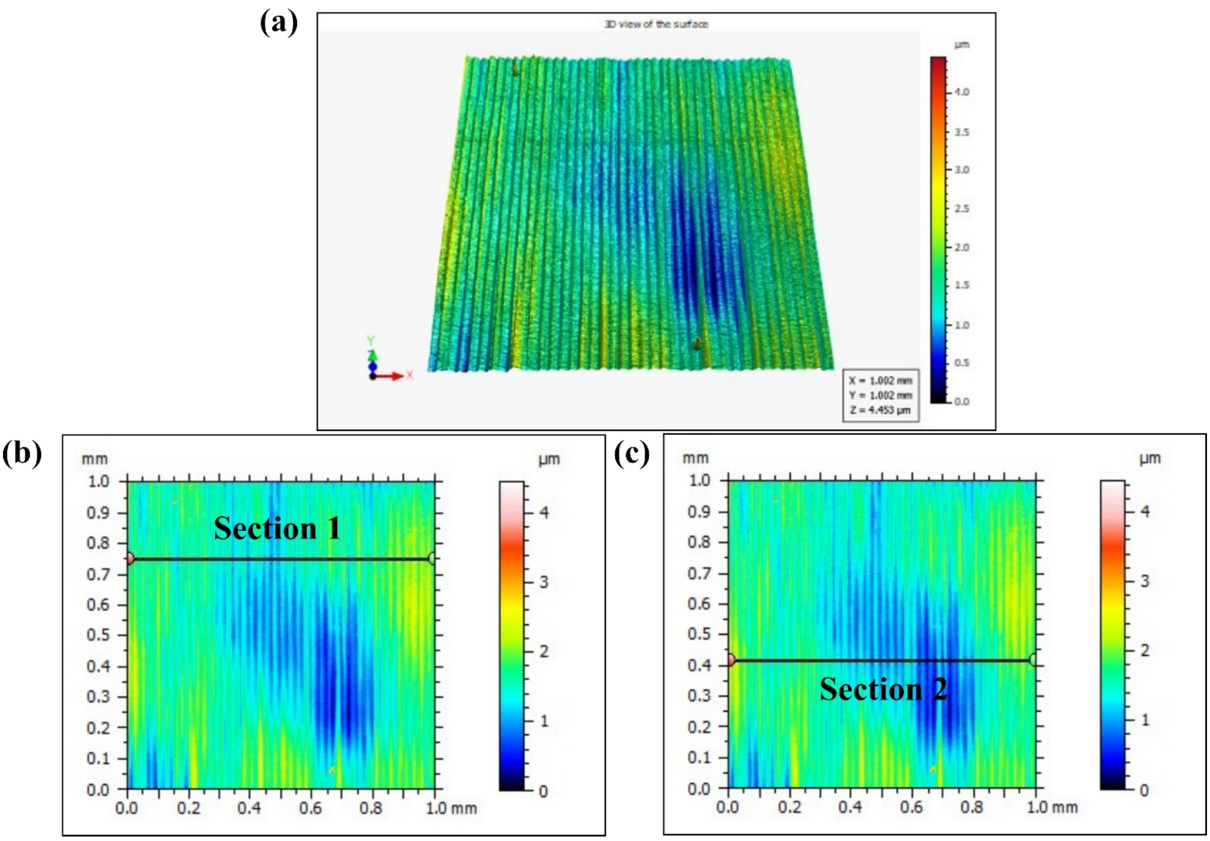

Figure. S3 (a) 3D image of copper tape surface, (b) 2D image of copper tape surface with measurement of roughness at section 1, and (c) 2D image of copper tape surface with measurement of roughness at section 2.

Table S1: The surface roughness value R_a (arithmeticmean deviation of absolute height) at section 1 and section 2.

Amplitude parameters	Value (µm)	
	At section 1	At section 2
R_a	0.2001	0.2149

3. The working mechanism of TENG

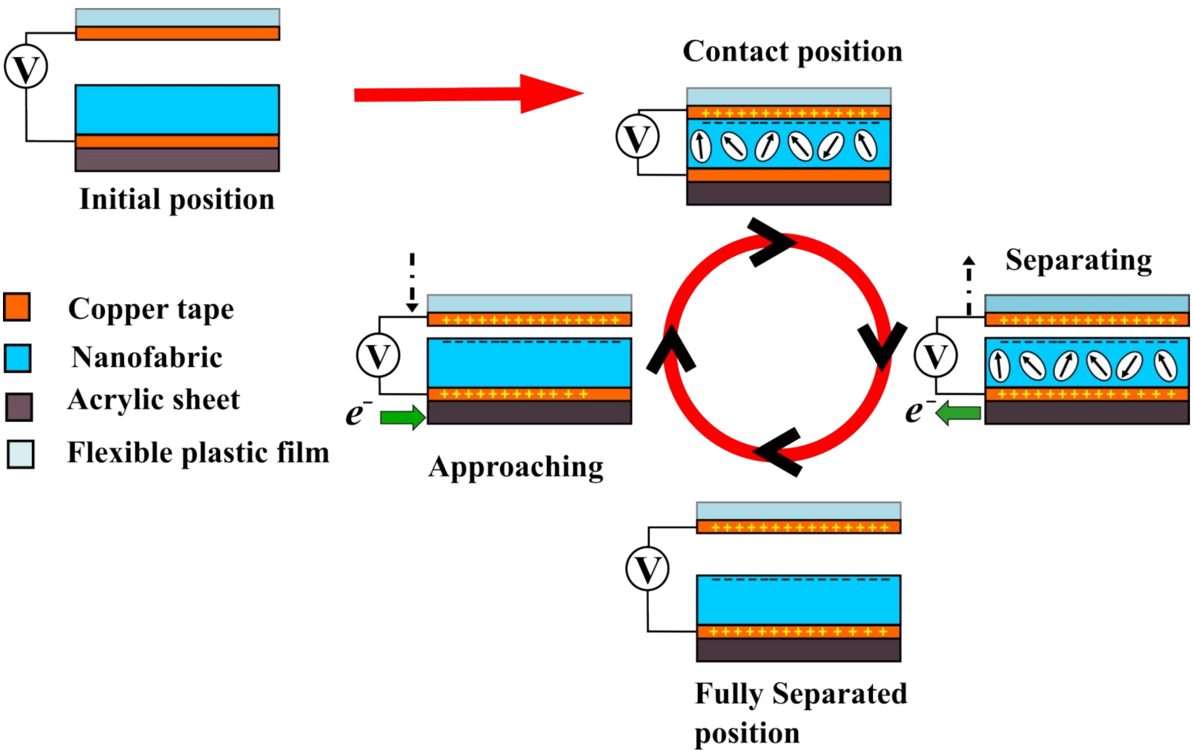

Figure. S4 Schematic of the working mechanism of TENG.

Figure S4 depicts the operational mechanism of the TENG. In a demonstration, the piezoelectric and triboelectric effects are combined to show that the piezoelectric effect also influences the triboelectric performance of the nanogenerator. The copper tape functions as a tribo-positive material by providing electrons, while the PVDF/MNS composite nanofabric serves as the tribo-negative one by accepting electrons. The upper copper electrode was located at a specific distance from the PVDF/MNS composite nanofabric in the initial configuration. The upper electrode does not come into contact with the bottom composite nanofabric due to the absence of external force, thus preventing the generation of charge across the electrodes. When an external force is applied, the upper electrode approaches the bottom composite nanofabric and makes contact with it. As a result of friction between two surfaces, triboelectric charges are generated at the interface. During contact, the piezoelectric nature of PVDF/MNS composite nanofabrics introduces charges, which contribute to the enhancement of triboelectric performance. Upon release of the external force, the upper electrode moves to the top due to the stiffness of the non-conducting polymer film, and charges generated due to the triboelectric effect will remain on the surface. The charges retained after the separation induce opposite charges on the electrodes through electrostatic induction. This induces a substantial electrical potential difference across the electrodes, triggering the flow of electrons through the external circuit to restore charge balance and generate an electrical signal. As soon as the TENG reaches its initial position, the potential difference reaches equilibrium, halting the flow of electrons. Once again, the application of an external force results in an opposite electrical potential difference, which allows electrons to flow back in reverse directions and creates an opposite signal [1–3].

4. ζ-potential of MNS

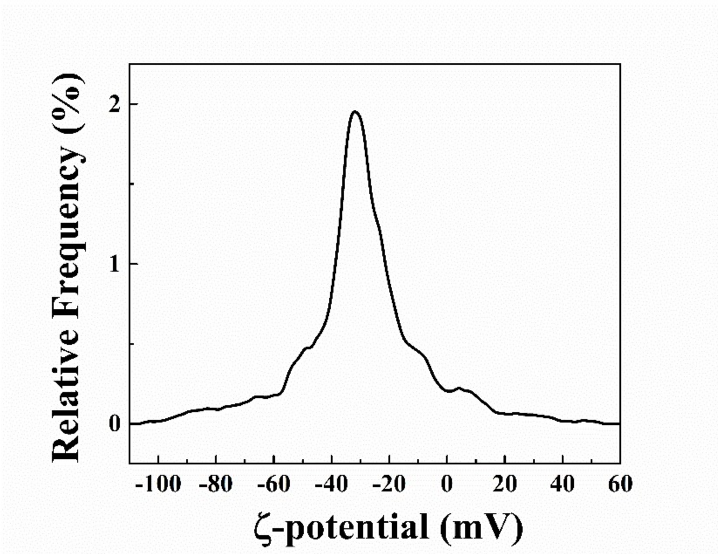

Fig. S5 ζ-potential curve of MNS with mean ζ-potential value of -33.4 mV.

References

1 S. Ippili, V. Jella, A. M. Thomas, C. Yoon, J. S. Jung and S. G. Yoon, *J. Mater. Chem. A*, 2021, **9**, 15993–16005.

2 B. Fatma, S. Gupta, C. Chatterjee, R. Bhunia, V. Verma and A. Garg, *J. Mater. Chem. A*, 2020, **8**, 15023–15033.

3 M. V. Paranjape, S. A. Graham, H. Patnam, P. Manchi and J. S. Yu, *Compos. Sci. Technol.*, 2022, **221**, 109323.